Production of Hyperons in Hydrogen by Positive Pions*

C. BALTAY, H. COURANT, W. J. FICKINGER, E. C. FOWLER, H. L. KRAYBILL, J. SANDWEISS, J. R. SANFORD,†‡ D. L. STONEHILL, AND H. D. TAFT

Yale University, New Haven, Connecticut, and Brookhaven National Laboratory, Upton, New York

INTRODUCTION

BETWEEN August 12 and 27, 1960, the 20-in. hydrogen bubble chamber of the Brookhaven National Laboratory bubble chamber group was exposed to electrostatically separated beams of positive pions produced by an external proton beam from the cosmotron. Table I summarizes the operating parameters of the exposure. Figure 1 indicates the trend of the π^+-p and π^--p total cross sections as a function of incident pion kinetic energy. The arrows point to the pion energies of this experiment.

A major objective of this experiment is the study of the reaction $\pi^++p\rightarrow\Sigma^++K^+$. The conservation laws of strangeness and charge require this to be the only way in which "strange particles" may be produced by positive pions on protons below the threshold energy for their production with an additional pion. The threshold kinetic energy for $\pi^++p\rightarrow\Sigma^++K^+$ is 891 Mev. A number of experiments, both with bubble chambers[1] and counters,[2] have been performed to study the production and decay of the Σ^+ hyperon. Two goals of the present experiment are to measure the cross section for the production of Σ^+ hyperons as a function of pion energy, and to examine by means of bubble chamber technique the asymmetry parameters for Σ^+ decay.[2] The longer run at 1.09 Bev has been made in order to test charge independence in production by comparison of cross sections for Σ^+ production by π^+ mesons on protons with those of Σ^- and Σ^0 production at the same energy by π^- mesons on protons.[3,4] Recently, it has been suggested by Michel[5] that for an angular interval where $(2\sigma_0)^{\frac{1}{2}}=(\sigma_+)^{\frac{1}{2}}+(\sigma_-)^{\frac{1}{2}}$ the polarizations of Σ^+, Σ^0, and Σ^- hyperons must be equal. This suggestion leads to the possibility of determining the sign of the asymmetry parameter α in Σ^+ decay relative to that in Λ^0 decay. This is a question of considerable interest which may be answered by combining the results of this experiment with those of Crawford and collaborators using the Berkeley 72-in. hydrogen bubble chamber.

At this time, results from two complete scans of the

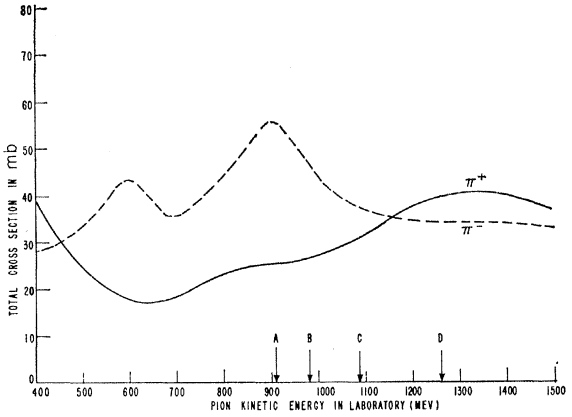

FIG. 1. Total cross sections for pion-proton interactions (T. J. Devlin *et al.*[9]) Point A is our π^+ run of 9160 photographs at 0.91 Bev. Points B–D are our runs of 9660, 85 150, and 7940 photographs at 0.98, 1.09 and 1.26 Bev.

TABLE I. Summary of Yale-Brookhaven π^+ experiment running conditions—August 12–27, 1960.

	Pion beam			
Lab KE (Bev)	0.91	0.98	1.09	1.26
Final ratio of pion track/beam tracks	95/100	94/100	92/100	90/100
Flux of useful beam tracks/frame	22.3	18.7	19.0	19.0
Number of useful frames (single count)	9160	9660	85 150	7940
	Cosmotron beam			
Lab KE of internal beam (Bev)	2.0	2.0	2.0	3.0
Internal beam intensity protons/pulse	3.0×10^{10}	4.0×10^{10}	5.0×10^{10}	1.5×10^{10}
Time between pulses (sec)	3.2	3.2	3.2	5.5
Accumulated running time (hr)	12	20	129	17

* This work was partially supported by the U. S. Atomic Energy Commission.

† Part of the work reported here has been included in a thesis which will be submitted by J. R. Sanford in partial fulfillment of requirements for the Ph.D. degree at Yale University.

‡ During part of this work J. R. Sanford held a National Science Foundation Cooperative Graduate Fellowship.

[1] J. L. Brown, D. A. Glaser, D. I. Meyer, M. L. Perl, and J. Van der Velde, Phys. Rev. **107**, 906 (1957); A. R. Erwin, Jr., J. K. Kopp, and A. M. Shapiro, *ibid.* **115**, 669 (1959); W. H. Hannum, H. Courant, E. C. Fowler, H. L. Kraybill, J. Sandweiss, and J. Sanford, *ibid.* **118**, 577 (1960); A. Berthelot, A. Daudin, O. Goussu, F. Grard, M. Jabiol, F. Levy, C. Lewin, A. Rogozinski, J. Laberrigue-Frolow, C. Ovannes, and L. Vigneron, preprint from Service de Physique Corpusculaire a Haute Energie, Centre d'Etudes Nucléaires de Saclay, France.

[2] B. Cork, L. Kerth, W. Wenzel, J. Cronin, and R. Cool, Phys. Rev. **120**, 1000 (1960).

[3] F. Crawford, R. Douglass, M. Good, G. Kalbfleisch, M. Stevenson, and H. Ticho, Phys. Rev. Letters **3**, 394 (1959).

[4] J. Sakurai, Phys. Rev. **107**, 908 (1957).

[5] L. Michel and H. Rouhaninejad, preprint from Laboratorie de Physique et Hautes Energies, BP 12, Orsay, S-et-O, France (1960).

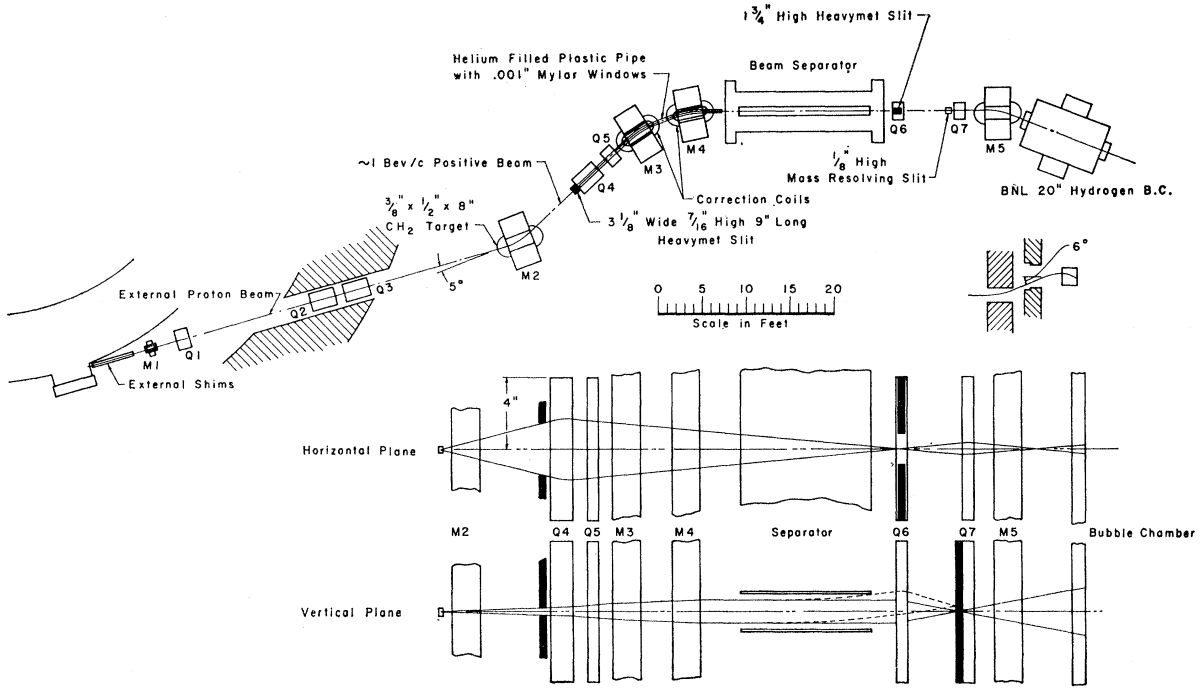

FIG. 2. Beam layout for the Yale π^+ experiment. A cosmotron quadrant is to the left of the upper drawing. External proton beam No. 2 comes to a focus just ahead of $M2$. The positive pion and inelastically scattered proton beam originates from the polyethylene target there. The momentum resolution is determined by the horizontal focus in $Q6$, and the mass separation is done in front of $Q7$. The lower two drawings show the horizontal and vertical envelopes of the beam.

entire exposure are in hand. Each event which is a possible example of Σ^+K^+ production has been analyzed in detail and definite identification has been made. An investigation of the flux, composition, and energy of the beam has been completed. This report provides results concerning:

(a) total Σ^+ production cross section as a function of the incident pion energy,

(b) differential Σ^+ production cross sections at three incident energies, and

(c) symmetry studies of Σ^+ decay.

Before presenting the results, it is necessary to describe some details of the techniques employed to aid in their evaluation.

EXPERIMENTAL

Separated π^+ Beam

Three of the authors (W. J. F., J. S., and J. R. S.) carried primary responsibility for the design and construction of Brookhaven Laboratory's first crossed-field separator. During the early part of this effort, M. Schwartz of Columbia University assisted the authors and the cosmotron staff. The separator is a large electromagnetic velocity spectrometer, consisting of two 15-×1-ft horizontal stainless-steel plates separated by 2.1 in. These plates are suspended by insulators inside a 36-in. diam×18½-ft long stainless-steel vacuum tank. Voltage can be applied to each plate, creating a vertical electric field. A horizontal magnetic field is provided by current coils located on the outside of the vacuum tank. The crossed-field separator at the cosmotron is quite similar to the separators built at the Lawrence Radiation Laboratory.[6] Operating conditions during this experiment (2.1-in. gap, 335 kv between the plates, tank pressure of 2×10^{-6} mm Hg, and electric field sparking rate of 5–10 sparks/hr) were also very much like those of its predecessors.

The basic difference between the separated π^+ beam at the cosmotron (see Fig. 2) and the K^- bevatron beam described by Eberhard *et al.*[7] is that one starts at the cosmotron with an external proton beam.[8] About 10^{10} protons/pulse traversed a ⅜-×½-×8-in. polyethylene target located just ahead of $M2$. The target's 8-in. dimension made an angle of about 7 deg with the proton beam. For each cosmotron pulse, the defining slit located in front of $Q4$ passed about 25 positive pions and 75 protons having the appropriate momentum and direction. The slit was 3⅛ in. wide by 7/16 in. high, and presented a solid angle to the target of 78×10^{-6} sr. The first 1-mil Mylar window of the helium bag was just

[6] W. Galbraith, Bevatron Note No. 288, Lawrence Radiation Lab., Berkeley, California (1957); J. J. Murray, University of California Radiation Lab., Rept. No. 9506 (1960).

[7] P. Eberhard, M. Good, and H. Ticho, Rev. Sci Instr. **31**, 1054 (1960).

[8] O. Piccioni, D. Clark, R. Cool, G. Friedlander, and D. Kassner, Phys. Rev. **98**, 275 (1955).

downstream of this slit. The helium bag extended to the beam entry port of the separator where there were two Mylar windows (one, 1 mil thick and the second, 8 mils thick). Quadrupole focusers $Q4$ and $Q5$ were arranged to give a beam which had nearly zero divergence in the vertical plane when it passed through the separator, and which converged horizontally to the center of $Q6$. Because of magnets $M3$ and $M4$ this was a dispersive focus. A momentum-defining slit was positioned in the center of $Q6$ and was adjusted to accept particles having a spread in momentum of $\pm 1\%$. The separator's magnetic field was adjusted to give no net deflection to the pions, while the slower protons were deflected upwards by 0.006 rad in the electric field of 66 kv/cm. After the separator, the pions and protons were brought to a vertical focus by $Q6$ a few inches ahead of $Q7$. At this focus the center of the pion image was separated from the proton image by about $\frac{3}{8}$ in. (see Fig. 3). Final mass selection was done at this point with an absorber of Hevimet containing a horizontal slit $\frac{1}{8}$ in. high. This slit transmitted about 20 useful pions and about 1 proton per pulse. The proton contamination never exceeded 7%, and the separation factor for our beam was 60.

Two special features of this beam design should be mentioned. First, the lack of homogeneity of the magnetic field in the main bending magnets $M3$ and $M4$ would have given rise to variations of vertical focal lengths for particles going down one side of the magnet compared to those going down the other side. This lack of homogeneity was overcome with special high-current coils placed inside the magnet gaps and energized up to 9600 amp-turns. Coils were used instead of iron pole face shims to facilitate changing the correction current as the excitation currents of the magnets were changed for the various parts of this experiment. Second, the 20-in. bubble chamber is photographed through its side and has a horizontal magnetic field. In order to place the low-momentum beam in the center of the chamber's beam window with a direction nearly parallel to the chamber walls, it was necessary to counteract the effect of the fringing magnetic fields which would have bent the beam downward by 9° before it entered the visible part of the bubble chamber. Most of this effect was cancelled by deflecting the beam upward 6° before it reached the bubble chamber magnet. This was achieved by rotating the last steering magnet ($M5$) 6° about the incident beam line. The magnet simultaneously gave the desired upward deflection and swept out the protons of degraded energy emerging from the final mass-defining slit.

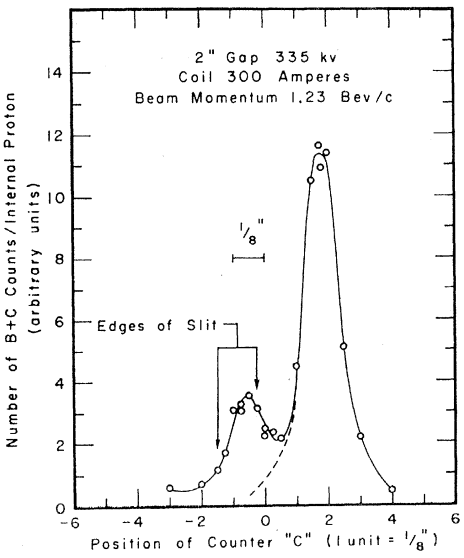

FIG. 3. A counter curve of the pion and proton images ahead of $Q7$ as the $\frac{1}{8}$-in. counter was moved up and down vertically through the images. The pion peak can be seen on the edge of the large proton peak.

The proton contamination in the final beam has been estimated by several methods:

(1) A scintillation counter of $\frac{1}{8}$ in. thickness traversed the beam at the position of the vertical focus and counted the number of particles in the images of the pions and protons. This counter was in time coincidence with two 2-×3-in. stationary scintillation counters a few feet down the beam. Figure 3 is a plot of the coincidence counts as a function of vertical position. The pion peak can be seen on the edge of the large proton peak, and the edges of the slit are indicated by the arrows.

(2) Variation of the separator magnetic field while keeping the full voltage on the plates swept the protons and pions across the mass-resolving slit. All tracks having the nominal beam direction in the bubble chamber were counted. Figure 4 is a plot of the number of tracks as a function of separator magnet coil current (or vertical position at the slit).

(3) The IBM 704 electronic computer was used to make kinematic fits of various primary track interpretations to a randomly selected sample of beam-initiated two-pronged events in the bubble chamber. Since the cross sections for p-p interactions at these momenta are well known,[9] this procedure gives a direct determination of the number of protons in the beam. It yields proton fractions of 2% at 0.91 Bev, 5% at 1.09 Bev, and 7% at 1.26 Bev as summarized in Table II. The other methods lead to numbers which are consistent with these values.

Chamber

The Brookhaven 20-in. hydrogen bubble chamber[10] with 17 000-gauss magnetic field was operated at a temperature of 25.02°K with $1\frac{1}{2}$-msec light delay to photograph a beam of 1-msec duration. This is different from

[9] S. J. Lindenbaum, Ann. Rev. Nuclear Sci. **7**, 317 (1957); T. J. Devlin, B. Barish, W. Hess, V. Perez-Mendez, and J. Solomon, Phys. Rev. Letters 4, 242 (1960).

[10] D. Rahm, report of Proceedings of International Conference on High Energy Accelerators and Instrumentation at CERN, Geneva, Switzerland (1959).

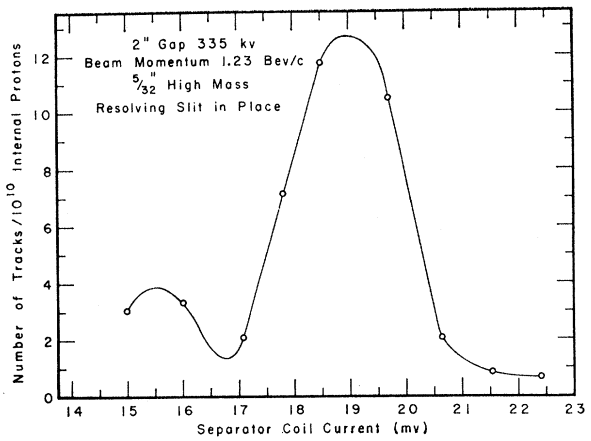

FIG. 4. The number of beamlike tracks in the bubble chamber as the pion and proton images were swept across the mass-resolving slit by the magnetic field of the separator.

previous operation[11] and avoided the use of the cosmotron rapid beam ejector without sacrificing the possibility of determining bubble density. The use of the rapid beam ejector at this time had been reducing the ejection efficiency at the cosmotron by a factor of 4.

The sensitive volume of the bubble chamber was photographed by four cameras in a 23-cm square array 88 cm to chamber's side. Each camera contained a 100-ft roll of Eastman Kodak Company's 35-mm Linagraph Ortho film.

Scanning and Measuring

Two stereographic views of the sensitive volume of the bubble chamber were scanned for Σ^+ production events. The scanners made sketches of these events, indicating how each one should be measured, and counted the number of beam tracks entering a reduced fiducial volume on every 10th frame. Figure 5 shows an example of Σ^+ production. The region marked on the photograph by white lines indicates the fiducial volume. All of the film has been scanned twice and the efficiency, based upon verified events, is summarized in Table III.

All events reported by the scanners were measured on digitized projection-type instruments. Three views of the event to be measured were mounted on a digitized stage. The x, y coordinates of any point on these films could be recorded on punched IBM cards. The least count of the digitizer corresponds to 1 μ on the film, and the over-all measurement accuracy on a track point is 3.5 μ on the film (35 μ in bubble chamber space). Event measurement consists of reading two fiducial marks in each

TABLE II. Summary of the data used to determine the pion/proton ratio. These data come from a study of two-pronged events in the bubble chamber.

Pion KE (Bev)	0.91	1.09	1.26
Corrected number of identified proton events	6	22	28
Total σ_{pp} used (mb)	27	37	46
Corrected number of identified pion events	353	339	325
Total $\sigma_{\pi p}$ used (mb)	26	31	40
No. of muons / No. of beam tracks	Not measured	3%[a]	Not measured
No. of pions / No. of protons	50/1	20/1	14/1
No. of pions / No. of beam tracks	95/100	92/100	90/100

[a] The muon contamination was estimated by counting "knock-on electrons" of energy too high to have been produced by beam pions.

[11] R. Louttit, report of Proceedings of Conference on Instrumentation for High Energy Physics at the University of California Radiation Laboratory, Berkeley, California (1960).

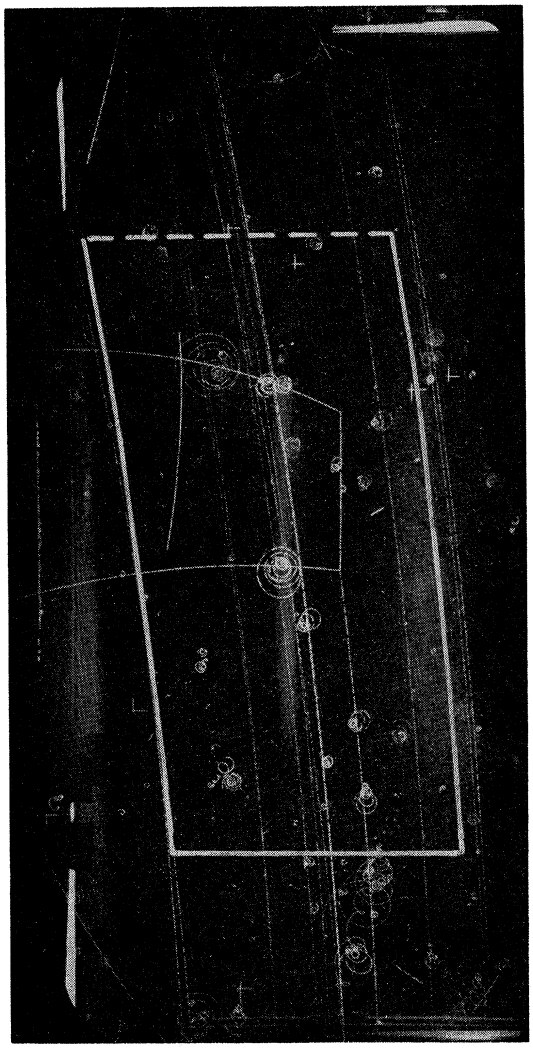

FIG. 5. This photograph of the sensitive volume of the 20-in. liquid-hydrogen bubble chamber contains an example of the reaction $\pi^+ + p \rightarrow \Sigma^+ + K^+$. The region outlined in white represents the fiducial volume used for total cross-section determinations.

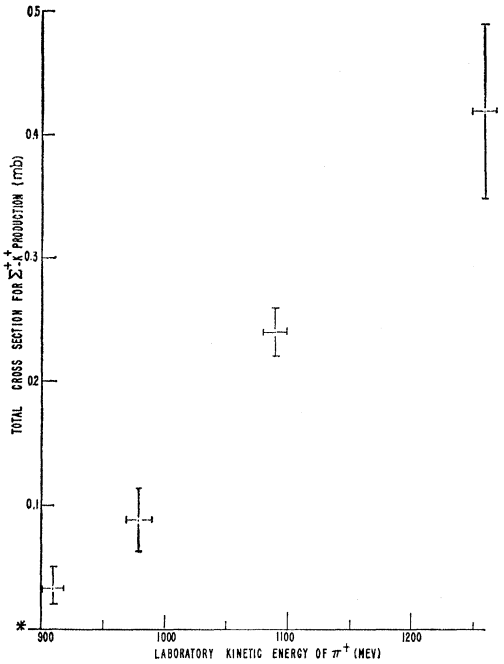

FIG. 6. This graph indicates how the total cross section for the reaction $\pi^+ + p \rightarrow \Sigma^+ + K^+$ depends upon incident pion kinetic energy as determined by this experiment.

of the three views, and the coordinates of each track in the best available pair of views.

Computing

The punched card output of the digitized measuring machines was fed into an IBM 704 electronic computer for further processing under the control of the Yale analyzer program YACK. This program performs a complete analysis of each event in a single pass and consists of two major sections.

The first section of the program utilizes a knowledge of the chamber geometry to perform an exact reconstruction of each measured point in three dimensions based on measurements in any arbitrary pair of cameras together with measurements of fiducial marks in the chamber. A helical spiral is then fitted through the measured points of each track and all relevant parameters such as momentum, coordinates, and space angles at both ends of each track are computed, together with the estimated average errors in these parameters. Since many of these quantities are mass dependent, the program allows up to six mass interpretations on each of a maximum of nine tracks. For the sigma-hyperon events, the decay track was interpreted both as a proton and as a π^+ throughout this section of the program. In addition, the first section computes the parameters of the beam track at the entrance window to the chamber, as well as a coplanarity volume for the first three tracks and a variable number of space angles.

The second section of the program performs a kinematic fit to any desired hypothesis by the method of least squares. A χ^2 figure representing the goodness of fit to each hypothesis is computed and used in the later analysis. Adjusted values of all relevant momenta and angles are also computed both in the laboratory and in the center of mass of the vertex being fitted. Analysis of the sigma-hyperon events proceeds first by fitting the production vertex to the reaction $\pi^+ + p \rightarrow \Sigma^+ + K^+$ where the measured beam momentum is replaced by a precise value based on many events and the measured sigma momentum is ignored. The fitted momentum and angles of the sigma are then propagated downstream to the decay vertex using known range-momentum relations, and the decay vertex is fitted both to the $\Sigma^+ \rightarrow \pi^+ + n$ mode and to the $\Sigma^+ \rightarrow \pi^0 + p$ mode. Before each fit, a missing mass and its error are computed and are compared with the expected values for this fit. If the computed value lies more than six standard deviations away from the expected value, the fit is skipped by the program.

TABLE III. Summary of the scanning results based upon two complete scans at each energy.

Pion KE (Mev)	Number of identified sigma events found in fiducial volume (events with short sigma tracks and small decay angles have been subtracted) First scan	Second scan	Total found as a result of two scans	Scanning efficiency (%)
910	4	4	5	94
980	8	12	12	100
1090	203	194	227	98
1260	37	32	37	100

Analysis

The results of the computer fitting of the event, the scanning sheet, and a photographic print of the event were inspected by a physicist. If the event fitted the production reaction $\pi^+ + p \rightarrow \Sigma^+ + K^+$ with a $\chi^2 < 12$ and if the Σ^+ decay fitted either $\Sigma^+ \rightarrow \pi^0 + p$ or $\Sigma^+ \rightarrow \pi^+ + n$ with a $\chi^2 < 6$, the event was considered to be satisfactorily measured. If the event could not be identified, it was remeasured. Mistakes in measurement and interpre-

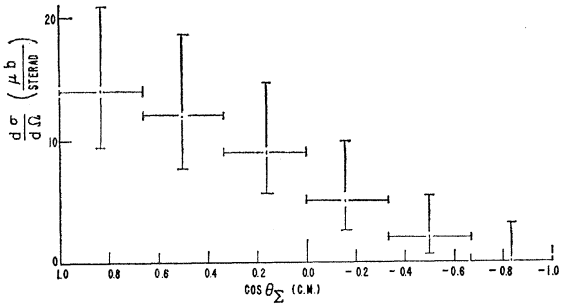

FIG. 7. The production differential cross section for the reaction $\pi^+ + p \rightarrow \Sigma^+ + K^+$ at an incident pion kinetic energy of 980 Mev.

tation were removed by this process. At the end of this reduction one had a collection of sigma events in the fiducial volume, a collection of sigma events outside the volume, and a group of events that were not Σ^+ production. Scanning losses of sigmas due to short lengths or small decay angles, or increased scanning efficiency for events where the K^+ stops, would produce biases in the angular distributions. Consequently, the raw number of events in each angular distribution interval (after removing events with sigma track length less than 0.4 cm and decay space angles less than 4°) were corrected for these effects. These corrected numbers were used to determine the scanning efficiencies. The resulting angular distributions have been normalized to the corrected number of events inside the fiducial volume.

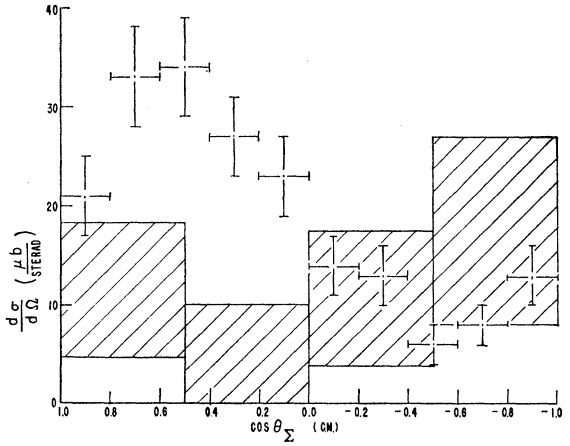

FIG. 8. The production differential cross section for the reaction $\pi^+ + p \rightarrow \Sigma^+ + K^+$ at an incident pion energy of 1090 Mev. The cross hatched regions are centered on the minimum cross sections for Σ^+ production predicted by charge independence using the $\pi^- + p \rightarrow \Sigma^0 + K^{0+}$ data of Crawford *et al.*[3]

RESULTS

Table IV and Fig. 6 show the total cross sections for production of Σ^+ hyperons for various incident pion energies. The previous experimental results[1] agree with these within the errors quoted. The results to date may

TABLE IV. Data used in the determination of the total cross sections for the reaction $\pi^+ + p \rightarrow \Sigma^+ + K^+$ at various energies.

Pion KE (Mev)	No. of events[a]	Length of pion beam scanned[b] (cm)	σ_T[c] (mb)
910	7	5.78×10^6	$0.033^{+0.018}_{-0.012}$
980	16.0	4.91×10^6	0.088 ± 0.026
1090	326.6	35.76×10^6	$0.25\ \pm0.02$
1260	51.1	3.33×10^6	$0.42\ \pm0.07$

[a] This is the raw number of events inside the fiducial volume from Table III corrected for scanning efficiency, sigma track lengths less than 0.4 cm, sigma decay angles less than 4°, and K^+ stopping detection efficiency.
[b] This is the raw number of beam tracks multiplied by the length of the fiducial volume, corrected for the pion fraction of the beam, the beam attenuation, and the beam criteria fraction.
[c] We used a liquid hydrogen density of 0.0618 g/cm³.

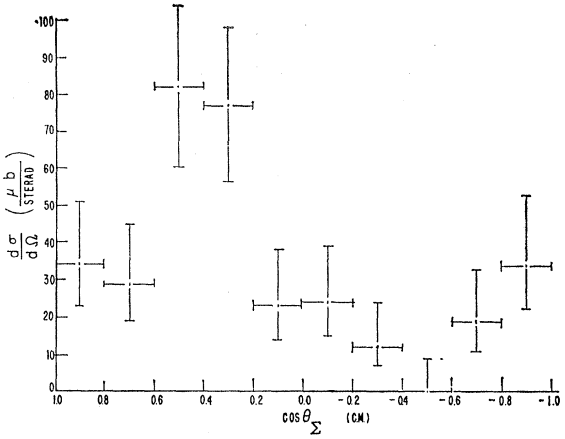

FIG. 9. The production differential cross section for the reaction $\pi^+ + p \rightarrow \Sigma^+ + K^+$ at an incident pion kinetic energy of 1260 Mev.

be summarized in a crude way by a straight line crossing the horizontal axis at the threshold (891.1 Mev). The horizontal error bars represent the limits of beam kinetic energy which include 90% of the beam tracks counted. The vertical error bars represent only the expected statistical fluctuations.

Figures 7–9 show the histograms which give the differential cross section as a function of the cosine of the center-of-mass angle for Σ^+ hyperon production for 980, 1090, and 1260 Mev, respectively. Again, the error bars represent the statistical error only. There were only seven examples of hyperon production at 910 Mev, so no angular data are presented for that energy.

Accepting these data at their face value, one sees a striking change in the angular distribution of the Σ^+ hyperons over the energies covered by this experiment. The forward peak seen at 980 Mev is not seen at 1090 Mev. At the latter energy, the results may be charac-

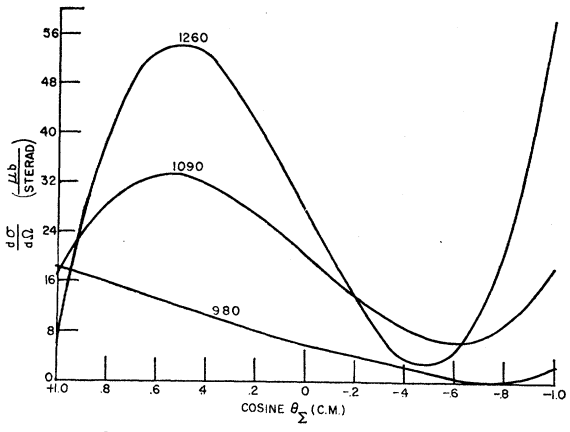

FIG. 10. These curves result from a least-squares fit of Legendre polynomials to the production differential cross sections. The upper curve is the best fit to the 1260-Mev data using polynomials through P_3. The middle curve is the fit to the 1090-Mev data through P_3, while the lowest curve fits the 980-Mev data using P_0, P_1, and P_2.

TABLE V. Distribution of decay pions with respect to the production plane for Σ^+ hyperons produced in π^+-p collisions at 1090 Mev.

Interval cm $\cos\theta_{\Sigma^+}$	$\alpha\bar{P}$	Standard deviation of $\alpha\bar{P}$	Experimentally obs N_{up}	Experimentally obs N_{down}	Predicted values[a] for $\alpha\bar{P}=+1.00$ (max possible) N_{up}	Predicted values[a] for $\alpha\bar{P}=+1.00$ (max possible) N_{down}
		π^+ decay				
-1.0 to -0.6	$+0.133$	0.26	8	7	11	4
-0.6 to -0.2	-0.105	0.23	9	10	14	5
-0.2 to $+0.2$	0.0	0.17	17	17	25	9
$+0.2$ to $+0.6$	-0.691	0.16	18	37	41	14
$+0.6$ to $+1.0$	$+0.122$	0.14	26	23	37	12
		π^0 decay				
-1.0 to -0.6	$+0.250$	0.26	9	7	12	4
-0.6 to -0.2	$+0.769$	0.33	9	4	10	3
-0.2 to $+0.2$	-0.133	0.18	14	16	23	7
$+0.2$ to $+0.6$	$+0.250$	0.15	27	21	36	12
$+0.6$ to $+1.0$	$+0.044$	0.15	23	22	34	11

[a] In order to emphasize the statistical limitations, the values for N_{up} and N_{down} for this experiment which would give $\alpha\bar{P}=+1.00$ are presented for comparison with the observed data.

terized by a peak near $\cos\theta_\Sigma=0.7$, with a minimum near $\cos\theta_\Sigma=-0.5$. The relative lowering of the cross section for forward angles and raising of that for backward angles appears at 1090 Mev and is stronger at 1260 Mev. Although the number of events is too small to allow curve fitting procedures to yield precise results, a least-squares fit of Legendre polynomials has been made. The main purpose here has been to reduce the data to curves in a consistent way. In each case, no more polynomials were used than the minimum needed to give the general shape. At 980 Mev, P_0, P_1, and P_2 were used; at 1090 and 1260 Mev, P_0, P_1, P_2, and P_3 were used. The results are shown on Fig. 10.

A major purpose of this experiment is the test of charge independence or conservation of isotopic spin in strong interactions involving strange particles. As discussed in previous papers,[1,2] if isotopic spin is conserved, then one expects three inequalities relating the three cross sections for Σ hyperon production in pion-proton collisions. These inequalities hold not only for the total cross sections for production but also for the differential cross sections. In the earliest experiments there was evidence of violation of the following inequality:

$$2(d\sigma/d\Omega)_{\Sigma^0K^0}\leqslant|[(d\sigma/d\Omega)_{\Sigma^-K^+}]^{\frac{1}{2}}+[(d\sigma/d\Omega)_{\Sigma^+K^+}]^{\frac{1}{2}}|^2.$$

Each of the shaded areas for four angular intervals in Fig. 8 is centered vertically on the value of the lower limit for hyperon production obtained by applying this inequality to the data of Crawford *et al.*[3] concerning Σ^-- and Σ^0-hyperon production at 1100 Mev. The vertical extent of each shaded area represents the error given in Crawford's values. It is concluded that, within quoted errors, charge independence is valid for these production processes.

Another major purpose of this experiment is to measure any asymmetry in the decay of the Σ^+ hyperon. If the Σ^+ is polarized along the normal to its plane of production and if its decay does not conserve parity, then there is an up-down asymmetry of the decay pion with respect to the original production plane. More specifically, the unit vector $\hat{n}$, normal to the plane of production is defined by

$$\hat{n}\equiv\mathbf{k}_1\times\mathbf{k}_2/|\mathbf{k}_1|\cdot|\mathbf{k}_2|\sin\theta_{12},$$

where $\mathbf{k}_1$ represents the momentum of the incoming beam particle and $\mathbf{k}_2$ represents the momentum of the produced Σ^+; both taken to be in the laboratory. The direction of the decay pion (positive or neutral) is given by its momentum vector $\mathbf{k}_3$ in the center-of-mass system of the Σ^+ hyperon. χ is defined as the angle between $\hat{n}$ and $\mathbf{k}_3$. If parity is not conserved in the decay process, one expects

$$d\sigma/d(\cos\chi)=1+\alpha\bar{P}\cos\chi$$

to give the angular distribution of the decay pions. α may vary from zero to one and is a measure of the lack of parity conservation. $\bar{P}$ is the average Σ^+ polarization for the interval of production angle being considered. It may be shown that (if $0<\chi<90°$ defines *up*, and $90°<\chi<180°$ defines *down*)

$$\alpha\bar{P}=2[(N_{up}-N_{down})/(N_{up}+N_{down})].$$

With the limited number of events available here, this evaluation of $\alpha\bar{P}$ has been used in five intervals of the production angle for events giving π^0p decays and five intervals for π^+n decays. The results are summarized in Table V.

These results are compatible with the hypothesis that $\alpha\bar{P}$ is zero. In order to make clear the limitations on the strength of such a conclusion, Table V shows the actual number of events in each category, the value and standard deviation for $\alpha\bar{P}$, and also the expected numbers in each category if $\alpha\bar{P}$ had its maximum possible value of 1.00.

CONCLUSIONS

(1) The rise of the cross section for Σ^+K^+ production with increasing incident energy indicates that both S- and P-wave production are important.

(2) The angular distribution of the Σ^+ particles changes rapidly with incident energy over the interval observed in this experiment. At 1090 and 1260 Mev the distributions require the presence of more than S- and P-wave angular momentum states. It is interesting to speculate as to whether some simple combination of S, P, and D wave may be found which will fit these data well.

(3) On comparing with previous results from π^- experiments, within experimental errors, our results for 1090 Mev are consistent with the hypothesis of charge independence. Indeed, it appears that there is a considerable angular interval for Σ^+'s in the backward hemisphere in which

$$(2\sigma_0)^{\frac{1}{2}}=(\sigma_+)^{\frac{1}{2}}+(\sigma_-)^{\frac{1}{2}}, \quad \text{approx.}$$

(4) For the 1090-Mev part of this experiment with a total of 327 Σ^+'s, there were 173 which decayed to π^++n and 154 which decayed to π^0+p. Within statistical errors, these decays are symmetrical with respect to the normal to the plane of Σ^+K^+ production. Since the previous bevatron counter study of parity conservation[2] in decay of Σ^+'s produced at 990 Mev gave the value of $\alpha\bar{P}_{\pi^0}=0.75\pm0.17$, we conclude that at 1090 Mev the polarization of the Σ^+'s is small. This change in polarization seems consistent with the considerable change in the angular distribution of the Σ^+'s between 980 and 1090 Mev observed in the present experiment, although as yet that question has not been investigated in detail.

ACKNOWLEDGMENTS

It is pleasing to call attention to the generous hospitality and technical assistance of the regular staff of the Brookhaven National Laboratory. The constant support of the Brookhaven bubble chamber group, headed by Dr. Ralph P. Shutt, and of the cosmotron department, headed by Dr. George Collins, made it possible to carry out this experiment. Dr. Robert Louttit was responsible for operation of the bubble chamber. The organization, scheduling, and coordination of the run itself was handled with the help of Dr. William Moore. The actual positioning of the magnets in the beam, arrangement of shielding, planning of safety precautions, etc., were primarily carried out by Al Schlafke and his staff. The operation of the cosmotron itself was maintained at peak efficiency by Ed Dexter and the operating group. The authors wish especially to thank Lou Potter and Ed Foster of the cosmotron department for their invaluable help on the long job of actual construction and operation of the parallel-plate separator. Bob Dryden and his staff at the A. G. S. provided regular instruction and help in keeping the separator's vacuum pumps in excellent operating condition.

The contributions to this work by all of the technical staff of the Yale group are gratefully acknowledged. Particular mention should be made of Horst Foelsche and Tom Ferbel, who shared in the actual run and played key roles in the scanning, measuring, and analysis of the photographs as well.

Finally, the authors wish to express their sincere thanks to the U. S. Atomic Energy Commission for its continued financial support of this work.

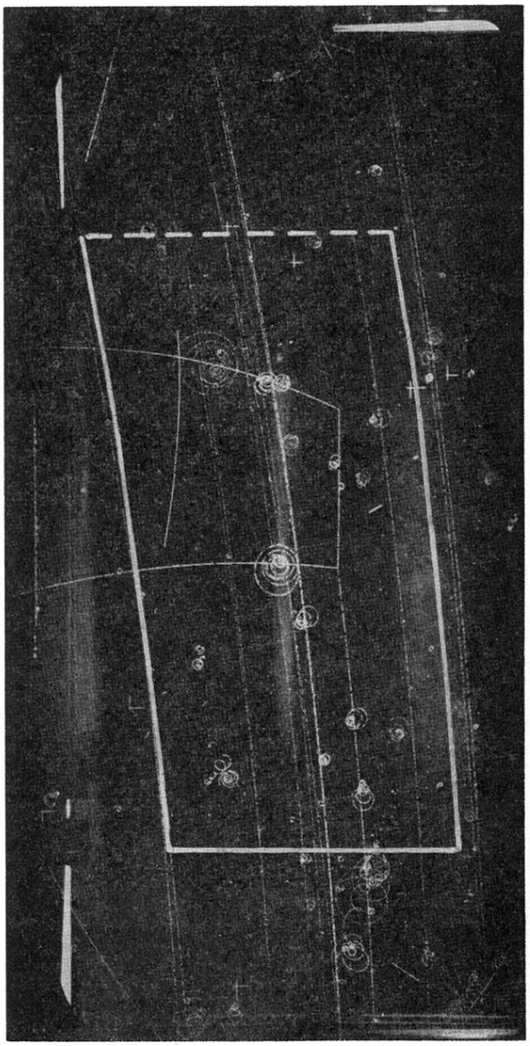

FIG. 5. This photograph of the sensitive volume of the 20-in. liquid-hydrogen bubble chamber contains an example of the reaction $\pi^+ + p \rightarrow \Sigma^+ + K^+$. The region outlined in white represents the fiducial volume used for total cross-section determinations.